

# Synthesis of Polymer Network Scaffolds from L-Lactide and Poly(ethylene glycol) and Their Interaction with Cells

Dong Keun Han<sup>†</sup> and Jeffrey A. Hubbell<sup>\*,‡,§</sup>

Biomaterials Research Center, Korea Institute of Science and Technology, P.O. Box 131, Cheongryang, Seoul 130-650, Korea, Division of Chemistry and Chemical Engineering, 210-41, California Institute of Technology, Pasadena, California 91125, and Department of Materials and Institute for Biomedical Engineering, ETH and University of Zürich, Moussonstrasse 18, Zürich, CH-8044 Switzerland

Received March 5, 1997; Revised Manuscript Received July 24, 1997<sup>®</sup>

**ABSTRACT:** New lactide-based poly(ethylene glycol) (PEG) polymer networks (GL-PEGs) have been prepared by UV photopolymerization using two nontoxic macromers, triacrylated lactic acid oligomer emanating from a glycerol center (GL) and monoacrylated PEG. These materials have been developed for use as polymer scaffolds in tissue engineering, which have cell-adhesion resistant, ligand-immobilizable, and biodegradable characteristics. The GL-PEG cross-linked polymer networks obtained were glassy and transparent, and the gel content was approximately 90%, irrespective of the degree of polymerization of lactide on the glycerol center and the amount and molecular weight of the PEG acrylate incorporated. All networks showed relatively low swelling in water, due to their highly cross-linked nature. They had no melting endotherms, but they displayed glass transition temperatures indicative of phase-mixing of the PEG. Analysis by ESCA, contact angle measurement, and cell culture indicated the presence of PEG at the network surfaces and showed that higher molecular weight PEG was incorporated into the network surfaces to a higher extent, rendered the surfaces more hydrophilic, and repelled cell adhesion more effectively than did PEG of lower molecular weights. All GL networks showed much less adhesion and spreading of human foreskin fibroblasts than glass used as a control. In particular, GL-PEG networks were highly resistant to cell adhesion due to the mobile PEG chains. Given that the terminal hydroxyl function on the incorporated PEG can be readily derivatized with a bioactive peptide, these degradable networks should be useful as polymer scaffolds for tissue engineering.

## Introduction

Tissue engineering applies the principles and methods of engineering, biology, and medicine toward the development of biological substitutes that restore, maintain, or improve function in normal and pathological tissues or organs.<sup>1</sup> A number of tissues and organs have been extensively investigated by this approach,<sup>2,3</sup> e.g., cartilage, skin, liver, bone, tendon, ureter, intestine, and blood vessels and peripheral nerves. Polymeric materials play an important role in tissue engineering and are being applied in conducting, guiding, and inducing tissue formation and in blocking tissue interactions.<sup>4,5</sup> Approaches in tissue engineering may be categorized into three types: hybrid systems of both biomaterials and living cells, systems of only cells without biomaterials that rely on biological processes to develop structure, and systems of only biomaterials without cells that rely on biological processes for cellular integration.<sup>6</sup> In particular, hybrid systems that combine biomaterials as structural scaffolds to organize living cells into a desired form have been studied extensively.<sup>5,6</sup> Polymers for these scaffolds should have nontoxicity, suitable biodegradability, good biocompatibility both prior to and during biodegradation, and the ability to interact specifically with appropriate cells.

Polyglycolic acid, polylactic acid, and their copolymers have been explored as biodegradable scaffolds because they ultimately degrade to natural metabolites. Scaf-

folds may be readily formed from these materials as bonded fibers or porous sponges.<sup>5,7</sup> These materials are relatively biocompatible and appropriately biodegradable, but they lack the ability to interact biospecifically with cells. To overcome this, biodegradable polydepsipeptides, alternating copolymers of  $\alpha$ -amino acids and  $\alpha$ -hydroxy acids, with functional side groups may be useful.<sup>8–10</sup> Recently, Langer and co-workers<sup>11</sup> have synthesized poly(lactic acid-co-lysine) by ring-opening copolymerization of lactide and a six-membered lysine-containing cyclic co-monomer. This biodegradable copolymer contained an amine group on the side chain of the lysyl residues to which a bioactive factor, such as the peptide arginine-glycine-aspartic acid (RGD),<sup>12</sup> can be grafted as a ligand to induce cell adhesion.

To be most useful as bioactive scaffolds, the base scaffold material should support little cell adhesion on its own; the cell adhesive properties of the scaffold can then be determined exclusively by the immobilized bioactive factor, and the possibility exists to develop materials which are adhesive to only targeted cell types.<sup>5</sup> To induce selective cell adhesion upon cell resistant scaffolds, reactive functional pendent groups on the material can be directly employed for grafting peptide ligands such as RGD, arginine-glutamic acid-aspartic acid-valine<sup>13</sup> in fibronectin, or tyrosine-isoleucine-glycine-serine-arginine<sup>14</sup> in laminin. For example, Cima<sup>15</sup> has prepared nondegradable cross-linked poly(ethylene glycol) (PEG) star hydrogels with high ligand capacity as matrices for coupling the desired cell-binding ligands.

PEG is a hydrophilic polyether and has received much attention for use in biomaterials, due to its low interfacial free energy with water, lack of charge, lack of binding sites for reactive proteins such as complement, high chain mobility, and steric stabilization effects.<sup>16</sup> It has been reported that PEG-treated biomaterials show

\* To whom correspondence should be addressed at the Institute for Biomedical Engineering, ETH and University of Zürich. Telephone: +41 1 632 45 75. Fax: +41 1 632 12 14. E-mail: hubbell@biomed.mat.ethz.ch.

<sup>†</sup> Korea Institute of Science and Technology.

<sup>‡</sup> California Institute of Technology.

<sup>§</sup> ETH and University of Zürich.

<sup>®</sup> Abstract published in *Advance ACS Abstracts*, September 15, 1997.

less protein adsorption<sup>17</sup> and platelet and cell adhesion<sup>18,19</sup> due to these characteristics. In addition, PEG has been used to reduce antigenicity and immune clearance of therapeutic proteins.<sup>20</sup>

Drumheller and Hubbell<sup>21</sup> have previously prepared low swelling, highly hydrophilic, cell-adhesion resistant, and/or biospecific cell adhesive semiinterpenetrating polymer networks by incorporating PEG–diacrylate and acrylic acid within a trimethylolpropyl triacrylate matrix. PEG in the network resisted protein adsorption and cell adhesion, but the very high cross-link density from the trimethylolpropyl triacrylate prevented swelling that would otherwise be induced by the high amount (up to 40%) of hydrophilic PEG. The acrylic acid groups incorporated into the network were useful as sites to immobilize RGD and other active peptides to promote cell adhesion. These materials exhibited ideal cell interaction characteristics for tissue engineering, but they were not biodegradable.<sup>22</sup>

In this work, we have extended our approach to novel networks that biodegrade into nontoxic products.<sup>23</sup> These polymer networks have been developed to enable scaffolds for use in tissue engineering and employ as components nontoxic glycerol, biodegradable L-lactide, and biocompatible and ligand-immobilizable PEG. Glycerol was used as an initiator for the ring-opening oligomerization of lactide to form an oligomeric triol, which was subsequently acrylated. This triacrylate was polymerized into a cross-linked network with a hydroxy-terminated monoacrylated PEG. The bulk and surface characteristics and cell interactions of these polymer networks have been evaluated.

## Experimental Section

**Materials.** L-Lactide was obtained from Aldrich and was recrystallized from ethyl acetate.  $\alpha$ -Monoacrylate- $\omega$ -monohydroxy poly(ethylene glycol)s (PEG–Ac) with molecular weights 1000 (PEG1K), 4000 (PEG4K), and 8000 (PEG8K) were purchased from Monomer-Polymer and Dajac and were dried by azeotropic distillation with benzene. Acryloyl chloride (AcCl) was obtained from Aldrich and was distilled before use. Glycerol (spectrophotometric grade, Aldrich), stannous octoate (St–oct, Sigma), triethylamine (TEA, Aldrich), and benzil dimethyl ketal (BDMK; 2,2-dimethoxy-2-phenyl-acetophenone, Aldrich) were used as received. All other chemicals were of reagent grade and were used without further purification.

**Synthesis of Glycerol–Lactide (GL) Triols.** Scheme 1 shows the synthetic reactions of GL triols and triacrylates. A typical example for synthesis of a GL triol is given as follows: a total of 1.53 g (0.017 mol) of glycerol (G), 21.6 g (0.15 mol) of L-lactide (L), and 0.3 g (0.74 mmol) of stannous octoate were added into a 100-mL round-bottomed flask equipped with a rubber septum and a magnetic stirring bar. The mixture was reacted in melt at 130 °C for 6 h under argon. The melt was allowed to cool and was dissolved in chloroform, microfiltered, and precipitated in hexane several times. The resulting product was dried under vacuum at 55 °C overnight to produce GL triol. The number of moles of lactide added per mole of glycerol for the various GL triols synthesized is shown in Table 1. The particular example illustrated above is for GL3. Yield: 92%. IR (CHCl<sub>3</sub>, cm<sup>-1</sup>): 3545 (hydroxyl), 1759 (ester). <sup>1</sup>H NMR (CDCl<sub>3</sub>):  $\delta$  1.56 (m, 3H, CH<sub>3</sub>), 2.85 (s, 1H, OH), 4.35 (m, 1H, L–CH–OH; 2H, CH<sub>2</sub>), 5.16 (m, 1H, L–CH; 1H, G–CH). <sup>13</sup>C NMR (CDCl<sub>3</sub>):  $\delta$  16.6 (CH<sub>3</sub>), 20.4 (terminal CH<sub>3</sub>), 62.5 (CH<sub>2</sub>), 66.6 (terminal CH), 69.0 (L–CH), 69.8 (G–CH), 169.5 (COO), 174.9 (terminal COO).

**Synthesis of Glycerol–Lactide (GL) Triacrylates.** As shown in Scheme 1, 20 g (14.4 mmol) of GL3 triol were dissolved in 200 mL of dichloromethane in a 500-mL round-bottomed flask and were cooled to 0 °C in an ice bath. A total of 8.74 g (86.4 mmol) of triethylamine and 7.82 g (86.4 mmol) of acryloyl chloride dissolved in 20 mL of dichloromethane were

## Scheme 1. Synthesis of GL Triacrylate

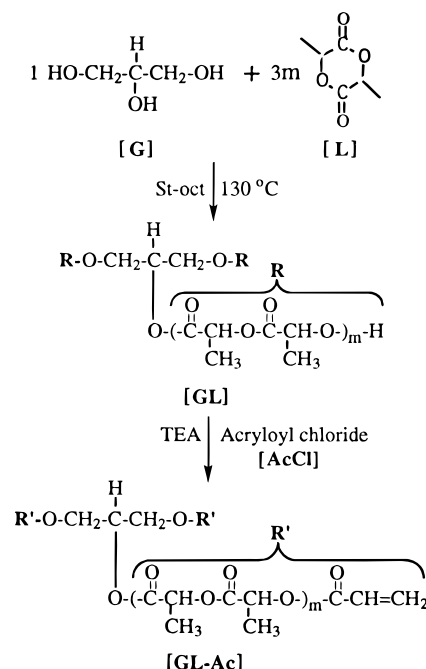


**Table 1. Synthesis and Degree of Substitution of GL Triols**

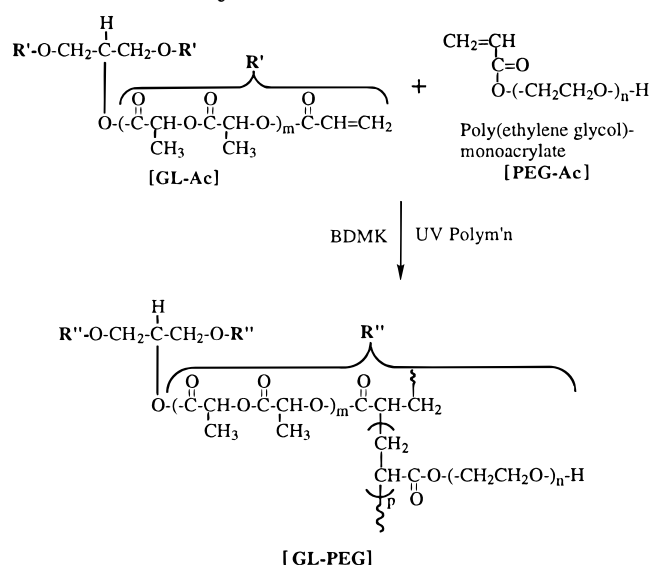
sample	[L]/[G] <sup>a</sup>	m <sup>b</sup>	[L]/[St–oct] <sup>c</sup>	appearance	DS (%) <sup>d</sup>	no. of arms <sup>e</sup>
GL1	3	1	200	viscous	89	2.7
GL2	6	2		viscous	93	2.8
GL3	9	3		waxy	100	3.0
GL5	15	5		solid	100	3.0
GL9	27	9		solid	100	3.0

<sup>a</sup> Molar ratio of lactide over glycerol. <sup>b</sup> Lactidyl repeating units that are the cyclic dimer of lactic acid. <sup>c</sup> Molar ratio of lactide over stannous octoate. <sup>d</sup> The conversion to GL triol from glycerol determined by <sup>1</sup>H NMR. <sup>e</sup> Average numbers of triol arms calculated from DS (%).

slowly dropped into the flask, and the mixture was reacted at 0 °C for 6 h and at room temperature for 42 h. The solution was microfiltered to remove triethylamine hydrochloride, and the filtrate was washed with dilute HCl and an aqueous NaHCO<sub>3</sub> solution to remove traces of triethylamine and HCl, respectively. The dichloromethane filtrate was then dried with anhydrous MgSO<sub>4</sub> and precipitated in diethyl ether and the precipitate dried under vacuum at room temperature overnight to produce triacrylated GL (GL–Ac; GL triacrylate). For the other GL triols, the same molar ratios were employed, i.e., 6 mol of acrylic acid and 6 mol of triethylamine per mole of GL triol. Yield: 83%. IR (CHCl<sub>3</sub>, cm<sup>-1</sup>): 1759 (ester), 1634 (double bond). <sup>1</sup>H NMR:  $\delta$  1.56 (m, 3H, CH<sub>3</sub>), 4.35 (m, 2H, CH<sub>2</sub>), 5.16 (m, 1H, L–CH; 1H, G–CH), 5.91–6.44 (m, 3H, CH<sub>2</sub>=CH). <sup>13</sup>C NMR (CDCl<sub>3</sub>):  $\delta$  16.6 (CH<sub>3</sub>), 62.5 (CH<sub>2</sub>), 68.4 (G–CH), 69.0 (L–CH), 127.5 (CH<sub>2</sub>=CH), 131.9 (CH<sub>2</sub>=CH), 169.5 (COO).

**Preparation of GL–PEG Networks.** Scheme 2 shows the synthetic reaction of GL–PEG polymer networks. A 25% w/v solution of 1 g (0.65 mmol) of GL–Ac, various amounts of PEG–Ac (10, 20, and 30 wt % of GL–Ac), and BDMK (1% w/w on the basis of GL–Ac plus PEG–Ac) dissolved in dichloromethane was prepared. The mixture was coated on the bottom of a Petri dish using an applicator and irradiated by a 100 W medium-pressure mercury ultraviolet source at an intensity of 10 mW/cm<sup>2</sup> (Blak-Ray Model B-100A, 365 nm, UV Products) to produce GL–PEG networks. The photocopolymerization was continued until gelation occurred. The resulting networks were denoted as follows: GL<sub>m</sub>–PEG<sub>n</sub>K–<sub>p</sub>, where, *m* (1, 2, 3, 5, and 9) is the number of repeats of lactide or dimeric repeats of lactic acid, *n* (1, 4, and 8) is the molecular weight (K = 1000) of PEG–Ac, and *p* (10, 20, and 30) is the

## Scheme 2. Synthesis of GL-PEG Networks



weight percent of PEG-Ac per GL-Ac. In addition, GL homonetworks were prepared using only GL-Ac in the absence of PEG-Ac for control.

**Characterization.** GL triols and triacrylates were analyzed by NMR, FTIR, and GPC.  $^1\text{H}$  and  $^{13}\text{C}$  NMR spectra were recorded on a GE Gemini 300 MHz spectrometer using deuteriated chloroform as a solvent. FTIR spectra were recorded on a Bruker IFS 66 spectrophotometer using chloroform as a solvent. GPC analysis was carried out at 35 °C using a Waters ALC/GPC 150 C equipped with micro-Styragel columns and calculated with polystyrene standards. Chloroform was used as an eluent at a flow rate of 1.0 mL/min.

The obtained GL and GL-PEG network films were dried under vacuum at 60 °C for 1 d, weighed (W1), and then extracted with chloroform at room temperature for 1 d, which was determined to be adequate for complete removal of unreacted PEG-Ac (data not shown). The films were dried again and weighed (W2). The gel content was calculated as  $(W2/W1) \times 100\%$ . Subsequently, the films were immersed in phosphate buffered saline (PBS, pH 7.4) at room temperature for 1 d and weighed (W3). The water absorption was calculated as  $[(W3 - W2)/W3] \times 100\%$ . Thermal analysis was performed using a Perkin-Elmer DSC 7 with a heating rate of 20 °C/min and a temperature range from -20 °C to +200 °C. Glass transition temperatures ( $T_g$ ) of PEG-Ac were not ascertained due to its very low  $T_g$  (about -70 °C). The elemental compositions of the network surfaces were determined using a S-Probe Surface Science ESCA spectrometer. The subpeaks of  $\text{C}_{1s}$  were deconvoluted using a curve-fitting method from a series of Gauss-Lorentzian curves. The advancing and receding contact angles were measured with a dynamic contact angle apparatus (DCA-315; Cahn Instruments) in water.

Human foreskin fibroblasts (HFFs) were obtained by collagenase digestion of neonatal foreskins and seeded prior to passage twelve onto the network films at 50 000 cells/cm<sup>2</sup> in Dulbecco's modified Eagle's medium (DMEM) supplemented with 10% fetal bovine serum (FBS), 400 U/mL of penicillin, and 400 mg/mL of streptomycin (all from GIBCO) at 37 °C in a 5% CO<sub>2</sub> incubator. After being seeded for 1 d, the films were fixed with 10% formaldehyde solution and then stained with 0.7% hematoxylin solution. At least five different fields at predetermined locations were counted at 200 $\times$  by phase contrast microscopy (Nikon) to determine the number of adhered cells. The ratio of the number of cells that adhered upon the film to the number of cells that were initially seeded was calculated as "% adhered cells".<sup>21</sup>

## Results and Discussion

**Synthesis of Triols and Triacrylates.** Table 1 lists synthesis conditions and degree of substitution (DS) of

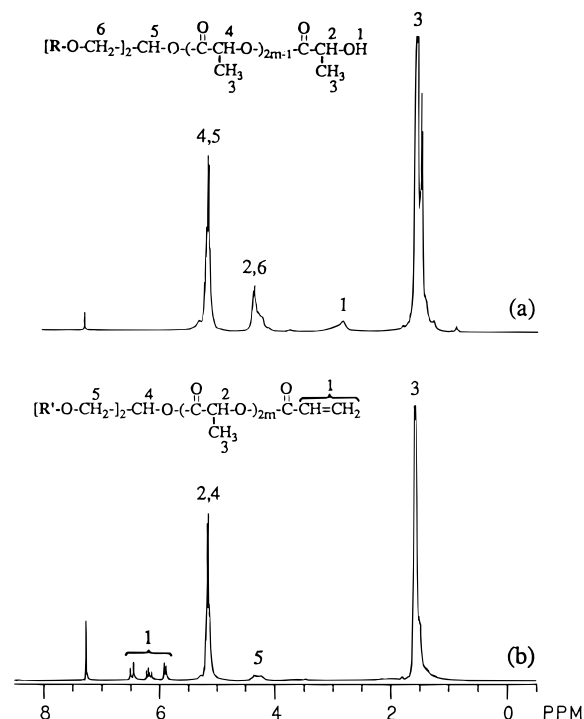


**Figure 1.**  $^1\text{H}$  NMR spectra of (a) GL3 triol and (b) GL3 triacrylate.

**Table 2. Molecular Weights of GL triols**

sample	theoretical	GPC	$^1\text{H}$ NMR
GL1	525	490	467
GL2	957	952	890
GL3	1389	1513	1389
GL5	2254	2674	2254
GL9	3984	4860	3984

the various GL triols that were synthesized. L-Lactide was ring-opening oligomerized using nontoxic glycerol as trifunctional initiator and stannous octoate as a catalyst to yield biodegradable nontoxic GL triol with nominally  $m$  lactidyl units or  $2m$  lactyl repeats per arm. Other investigators have synthesized various biodegradable diols,<sup>19,24</sup> triols,<sup>25,26</sup> and tetraols<sup>26,27</sup> containing lactides using ring-opening polymerization. In this study, five types of GL triols were synthesized by controlling the molar ratio of lactide to glycerol from GL1 to GL9. When the ratio was above 9, or three lactidyl units per glycerol arm, DS, the conversion to GL triol from glycerol, was 100% from  $^1\text{H}$  NMR spectra (Figure 1), obtained specifically by measurement of the disappearance of  $\text{G}-\text{CH}_2\text{OH}$  ( $\delta$  3.73) and the ratio of  $\text{L}-\text{CH}$  ( $\delta$  5.16) to  $\text{L}-\text{CH}-\text{OH}$  ( $\delta$  4.35). This suggests that each of the three hydroxyl groups of glycerol initiated the polymerization of L-lactide. The molecular weights of GL triols were compared with theoretical values, GPC, and proton NMR, as shown in Table 2. The results of GPC and NMR regarding molecular weight were very similar to the theoretical value, again indicating that the reaction proceeded to near completion.

Triacrylates were synthesized by reacting GL triols with acryloyl chloride.<sup>19,26</sup> It was found from  $^1\text{H}$  NMR spectra (Figure 1) that the DS of GL triol to triacrylates was also 100%, specifically obtained by measurement of disappearance of  $\text{L}-\text{OH}$  ( $\delta$  2.85) and the ratio of  $\text{Ac}-\text{CH}_2=\text{CH}$  ( $\delta$  5.91-6.44) to  $\text{L}-\text{CH}_3$  ( $\delta$  1.56). This demonstrates that each terminal hydroxyl group in the GL triol was completely derivatized with a polymeriz-

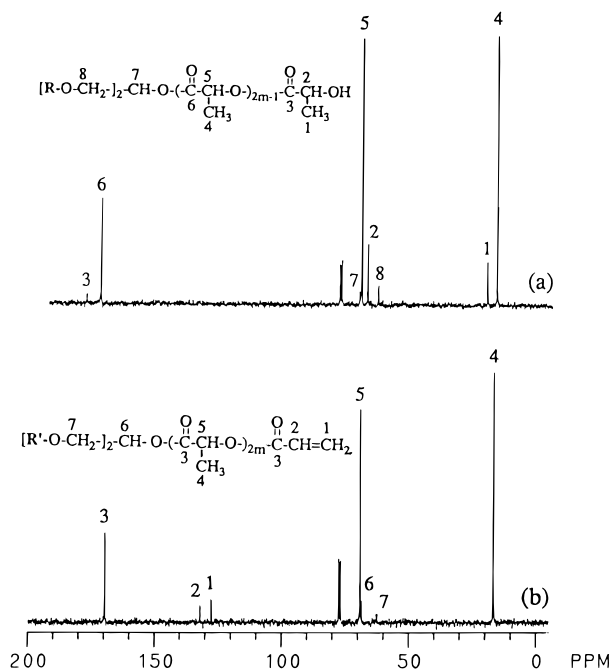


**Figure 2.**  $^{13}\text{C}$  NMR spectra of (a) GL3 triol and (b) GL3 triacrylate.

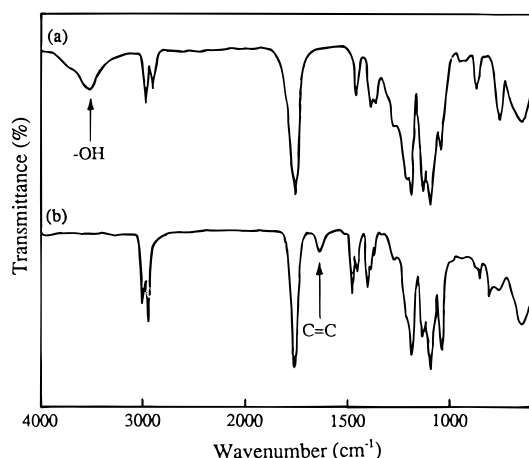


**Figure 3.** FTIR spectra of (a) GL3 triol and (b) GL3 triacrylate.

able acrylate group. Each chemical structure of the triols and triacrylates was also characterized with  $^{13}\text{C}$  NMR and FTIR. Figure 2 shows representative  $^{13}\text{C}$  NMR spectra of GL triol and triacrylate. Triacrylates were confirmed by the presence of a vinyl group at 128 and 132 ppm and by the disappearance of terminal lactide carbons at 20.4, 66.6, and 174.9 ppm. From FTIR results as shown in Figure 3, while the hydroxyl group from the triol completely disappeared at 3545  $\text{cm}^{-1}$  for GL triacrylate, a vinyl group by acrylation was revealed at 1634  $\text{cm}^{-1}$ .

**Bulk Properties of GL-PEG Networks.** Polymer networks were formed from the two reactive macromers, GL-Ac and PEG-Ac, at various mass ratios. These macromers were photocopolymerized using a simple UV source with the initiator BDMK to form cross-linked networks. Durations of UV irradiation for GL-PEG networks ranged from 30 s to 5 min, depending on the film thickness. The obtained network films were glassy and transparent.

Table 3 lists bulk properties of GL-PEG networks. Two series of GL3 and GL9 networks were prepared to

**Table 3. Bulk Properties Data of GL-PEG Networks**

sample	gel content (%) <sup>a</sup>	water absorption (%) <sup>b</sup>	$T_g$ (°C) <sup>c</sup>
GL3 network	88	3.6	61
GL3-PEG1K-20	89	14	40
GL3-PEG4K-10	90	15	41
GL3-PEG4K-20	87	21	39
GL3-PEG4K-30	87	25	36
GL3-PEG8K-20	89	30	37
GL9 network	94	1.0	67
GL9-PEG1K-20	93	6.2	49
GL9-PEG4K-10	92	3.9	48
GL9-PEG4K-20	88	8.5	44
GL9-PEG4K-30	88	16	40
GL9-PEG8K-20	90	19	40

<sup>a</sup> Gel content = (weight after chloroform extraction/weight before chloroform extraction)  $\times$  100%. <sup>b</sup> Water absorption = [(weight after 1 d swelling in PBS - weight after chloroform extraction)/weight after 1 d swelling in PBS]  $\times$  100%. <sup>c</sup> Determined by differential scanning calorimetry.

change their degradation rate (not characterized in this study). The gel content of the networks which were formed by cross-linking was between 87 and 94% regardless of the identity of the GL triacrylate and the incorporation and content of PEG-Ac. After chloroform extraction, the sol content of items such as unreacted macromers and homopolymers was about 10%.

Water absorption within the GL-PEG networks was evaluated by differential weight measurements. The GL3 series, containing a smaller amount of lactyl ester than the GL9 series, showed higher water absorption. Water absorption within the GL networks increased as PEG was incorporated, as the PEG molecular weight was increased, and as the PEG content was increased, implying more hydrophilicity. The increase in water absorption with PEG-Ac molecular weight was more substantial in the GL3-PEG networks than in the GL9-PEG networks. The increase in water absorption with PEG-Ac content was rather modest and was greater in the GL3-PEG network than in the GL9-PEG network. Overall, the extent of water absorption was relatively small, the maximum value being only 30%. These results indicate that the GL-PEG networks synthesized should have better mechanical strength for use in many tissue engineering applications than hydrogels of equivalent cell nonadhesiveness.

The thermal behavior of GL and GL-PEG networks was examined by DSC. All GL and GL-PEG networks had no melting endotherms ( $T_m$ ) because the GL and PEG macromers were completely polymerized to form the cross-linked networks. In particular, the lack of a PEG  $T_m$  indicates that the PEG was distributed throughout the network and was not separated into PEG-rich phases. Drumheller and Hubbell<sup>22</sup> reported that grafted semi-IPNs formed with PEG-diacrylate had no melting endotherms, unlike semi-IPNs formed with PEG-diacetate and PEG-diol, by virtue of an absence of PEG-rich crystalline domains and a high degree of phase mixing with the comonomer. Thus, PEG in GL-PEG networks was phase mixed within the network bulk to a high degree, because one side of the PEG was covalently grafted within the network. GL and GL-PEG networks, however, exhibited a glass transition temperature ( $T_g$ ) due to the loose cross-linking by means of the oligolactyl spacer. The GL9 series showed higher  $T_g$  than the GL3 series at equivalent PEG-Ac content and molecular weight because the GL9 series has a higher content of rigid lactide groups. All GL-PEG networks also showed lower  $T_g$  than did the GL homo-

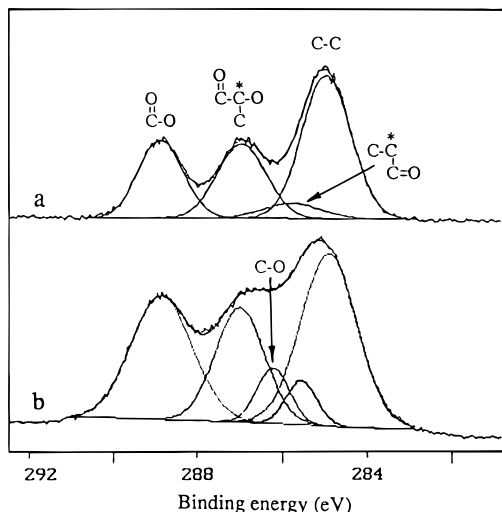


**Figure 4.** High-resolution ESCA spectra of  $C_{1s}$  of (a) the GL3 network and (b) the GL3-PEG4K-20 network.

networks, and the  $T_g$  of GL-PEGs decreased with increasing PEG molecular weight and with increasing PEG content, as listed in Table 3. These results reveal that as PEG is incorporated within the networks, the bulk becomes more rubbery and soft.

**Surface Properties of GL-PEG Networks.** The atomic surface compositions of the network films were determined by ESCA. Figure 4 shows characteristic high-resolution  $C_{1s}$  ESCA spectra of GL and GL-PEG networks. It has been reported that lactide polymer indicates three distinct peaks in  $C_{1s}$ , namely aliphatic carbon (C-C) at 285.0 eV, methine carbon [C(O)C\*(C)O] at 287.1 eV, and carbonyl carbon (C=O) at 289.1 eV.<sup>28</sup> GL homonetworks showed four peaks, the three indicated above plus one deriving from the vinyl group [CC\*C(O), 285.7 eV] introduced by acrylation of the GL triols. Five  $C_{1s}$  peaks appeared for all GL-PEG networks, the additional peak resulting from the ether group (C-O, 286.5 eV) of the incorporated PEG.<sup>29</sup> Table 4 lists the summarized atomic composition and results from peak fitting of ESCA  $C_{1s}$  spectra for the GL and GL-PEG networks. After the incorporation of PEG in the GL networks, the oxygen atomic percent of the GL-PEG increased at the expense of a decrease in the carbon atomic percent.

Peak-fitting analysis was performed to examine the PEG content of the network surfaces. The ether-bonded carbon peak derives exclusively from the PEG-Ac. One may thus consider the fraction of total carbon that is ether-bonded carbon (286.5 eV) as indicative of the degree of presence and surface enrichment of PEG at the surface of the GL-PEG networks. The theoretical carbon atomic percents of the GL network are 61% and 60% for GL3 and GL9 respectively. Considering the PEG-Ac carbon atoms as exclusively ether-bonded, the theoretical fractions of carbon that would be ether-bonded in the GL3-PEG network would be 12%, 22%, and 32% for networks with 10%, 20%, and 30% PEG-Ac, respectively, and for the GL9-PEG network 11%, 22% and 32%, respectively. From the peak-fitting analysis, by comparison with the values shown in Table 4, one may thus reach the following conclusions. It is unequivocal that PEG was present at the surface of the GL-PEG networks, accounting for a considerable fraction of the surface carbon. It is also clear, however, that the PEG was present at the surface in lower amounts than theoretical. This may indicate that the degree of

incorporation of the (mono)acrylated PEG into the gel fraction was lower than that of the (tri)acrylated GL macromer (the bulk network composition was not measured), i.e., that the approximately 10% of macromer mass that was extractable from the GL-PEG networks after polymerization was composed largely of PEG-Ac or that the surface PEG was somewhat buried into the polymer in the high-vacuum environment of the ESCA spectrometer. It is also clear that the higher molecular weights of PEG-Ac were more effective in imparting chemical evidence of their presence than were smaller molecular weights of PEG. It is not possible from the present studies to determine if this relates to increased chemical incorporation or to lower diffusive mobility of the higher molecular weight PEG-Ac.

The physicochemical presence of the PEG at the surface of the GL-PEG networks was clearly observable. The surface wettability of the network films was evaluated by measuring dynamic contact angles in water as listed in Table 5. GL homonetworks showed relatively hydrophobic surfaces as compared with GL-PEG networks, and the GL9 series was more hydrophobic than the GL3 series due to the higher content of lactide groups. The GL9-PEG networks were rendered less hydrophilic by the incorporation of PEG than were the GL3-PEG networks, presumably also due to the higher lactide content of the GL9 vs the GL3 base networks. The hydrophilicity increased with increasing PEG content for the GL-PEG networks, as would be expected, this is and consistent with the surface analysis by ESCA. At constant mass fraction PEG-Ac in the comonomer mixture, higher molecular weights of PEG-Ac were more effective in rendering the GL-PEG network surface hydrophilic than were lower molecular weights, also consistent with the analysis by ESCA. In addition, after hydration in phosphate-buffered saline (pH 7.4) for 1 d, the hydrophilicity was considerably increased as compared with the same sample before hydration. Thus, the GL-PEG network surfaces would seem to be capable of extensive rearrangement on a relatively slow time scale in an aqueous environment.<sup>30</sup> Both the GL and the GL-PEG networks were capable of such rearrangement, but the effect was much more pronounced in the PEG-containing network. The PEG chains, terminally tethered into the network by only one end, would be expected to be capable of extensive rearrangement. The dependence of this rearrangement on PEG content or molecular weight was not explored. Contact angle hysteresis values ( $\Delta\theta = \theta_{adv} - \theta_{rec}$ ), which may relate to many factors including surface roughness, patchwise heterogeneity, deformation, liquid penetration and swelling, short time scale surface reorganization, and mobility of chains,<sup>31</sup> were similar on all materials tested.

**Cell Repellency of GL-PEG Networks.** Human fibroblasts were cultured upon the various polymer networks to evaluate their resistance to cell adhesion. Figure 5 shows typical micrographs of fibroblasts cultured for 1 d on glass (as a reference standard), the GL9 network, and the GL9-PEG4K-20 network. The GL-PEG networks in general showed less adhesion and spreading of HFFs than did GL homonetworks and much less than did glass.

Figures 6 and 7 show the summarized results of HFF adhesion onto the GL3 and GL9 series, respectively. GL9-PEG networks displayed nearly the same fibroblast adhesion as GL3-PEG ones. As the content of PEG at constant molecular weight was increased, less

**Table 4. ESCA Data for GL-PEG Networks**

carbonyl sample	surface atomic %		atomic % of C <sub>1s</sub> high resolution <sup>a</sup>				
	C	O	aliphatic C-C	vinyl C-C*-C=O	ether C-O	methine O=C-C*(-C)-O	O=C-O
			285.0 eV	285.7 eV	286.5 eV	287.1 eV	289.1 eV
GL3 network	69	31	47	5.8	0	24	24
GL3-PEG1K-20	60	40	35	5.6	6.1	27	27
GL3-PEG4K-10	61	39	37	5.5	6.9	25	26
GL3-PEG4K-20	62	38	37	5.3	7.1	25	25
GL3-PEG4K-30	63	37	38	5.2	12	23	23
GL3-PEG8K-20	64	36	39	5.1	13	21	22
GL9 network	72	28	51	4.8	0	22	22
GL9-PEG1K-20	64	36	39	4.2	4.3	26	27
GL9-PEG4K-10	64	36	39	4.3	6.3	25	26
GL9-PEG4K-20	65	35	41	4.1	7.5	24	24
GL9-PEG4K-30	67	33	44	4.0	8.0	22	22
GL9-PEG8K-20	67	33	44	3.8	9.2	22	22

<sup>a</sup> The asterisk corresponds to the analyzed carbon.

**Table 5. Dynamic Contact Angles<sup>a</sup> for GL-PEG Networks**

sample	$\theta_{adv}$	$\theta_{rec}$	hysteresis
GL3 network	83	54	29
GL3 network <sup>b</sup>	72	39	33
GL3-PEG1K-20	79	50	29
GL3-PEG4K-10	74	47	27
GL3-PEG4K-20	63	39	24
GL3-PEG4K-30	56	30	26
GL3-PEG4K-30 <sup>b</sup>	45	10	35
GL3-PEG8K-20	50	26	26
GL9 network	92	58	34
GL9-PEG1K-20	85	55	30
GL9-PEG4K-10	78	50	28
GL9-PEG4K-20	73	45	28
GL9-PEG4K-30	69	42	27
GL9-PEG8K-20	67	40	27

<sup>a</sup>  $\theta_{adv}$  = advancing contact angle;  $\theta_{rec}$  = receding contact angle; hysteresis =  $\theta_{adv} - \theta_{rec}$ . <sup>b</sup> After hydration in PBS (pH 7.4) for 24 h.

HFF adhesion was observed. Furthermore, as the molecular weight of the PEG was increased, the resistance of the GL-PEG network to cell adhesion was also increased. Both of these trends were observed on both the GL3-PEG and GL9-PEG networks, consistent with the measurements of wetting by DCA. It has been reported that cell interactions with substrates bearing PEG depend on the PEG molecular weight/chain mobility,<sup>32,33</sup> PEG-phase mixing/separation,<sup>22,34</sup> and surface hydration.<sup>33</sup> GL-PEG networks not only have pendent PEG grafted on their backbone but also are somewhat PEG phase mixed so that the mobile PEG chains may readily reorganize toward the interface in water, as demonstrated by DCA measurements after hydration in buffered saline. Therefore, the cell repellency of the GL-PEG networks may be attributed to the incorporation and high molecular weight of PEG.

It is generally well-known that PEG may be incorporated into substrates by a variety of methods to improve their biocompatibility. The methods include physical adsorption<sup>35</sup> and entrapment,<sup>36</sup> covalent coupling in the main<sup>37</sup> or side<sup>29,30</sup> chain, photoinduced grafting,<sup>38</sup> glow discharge treatment,<sup>39</sup> and  $\gamma$ -irradiation.<sup>16</sup> Such PEG-containing materials have been reported to have low protein adsorption<sup>13</sup> and cell adhesion as described more extensively above. Drumheller and Hubbell<sup>21,22</sup> previously reported the excellent resistance to cell adhesion of PEG-containing cross-linked polymer networks, but they employed materials that did not result in biodegradation. The subject GL-PEG networks of this study were based on a similar approach to obtain a network that was highly resistant to cell adhesion as well as fully

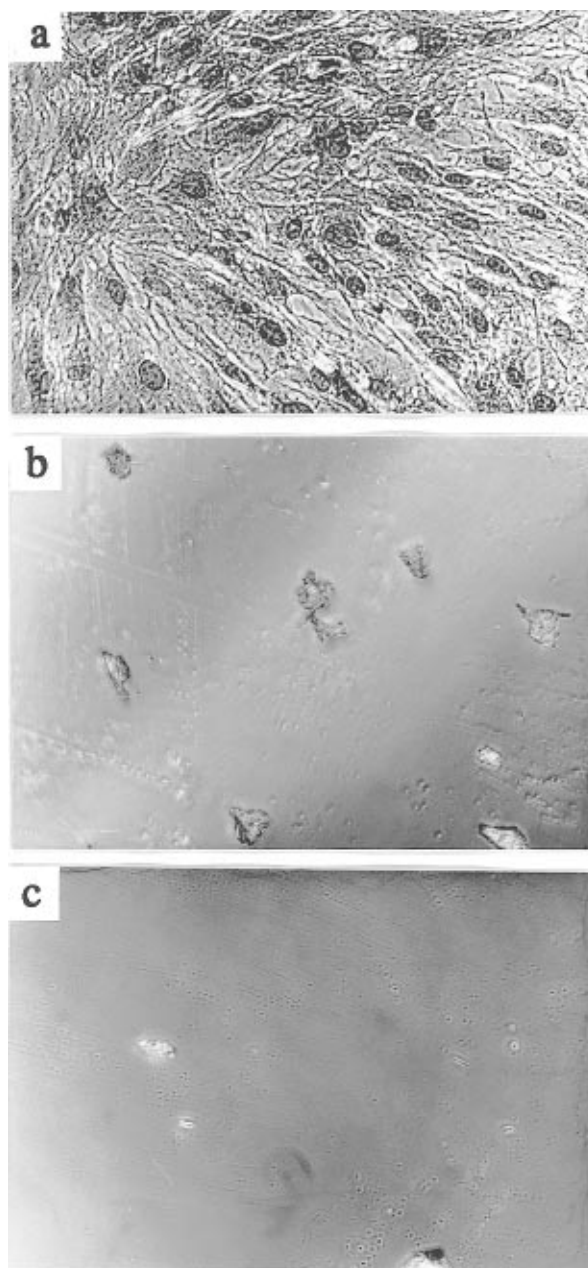


**Figure 5.** Micrographs of fibroblast adhesion after culturing for 1 d on (a) glass, (b) the GL9 network, and (c) the GL9-PEG4K-20 network (200 $\times$ ).

biodegradable. The biodegradation rate of GL-PEG networks can be potentially controlled from several days

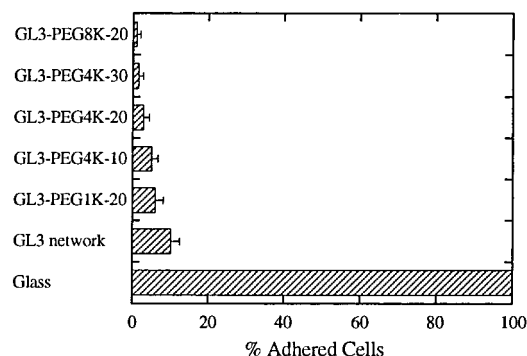


Figure 6. Fibroblast adhesion onto GL3-PEG networks.

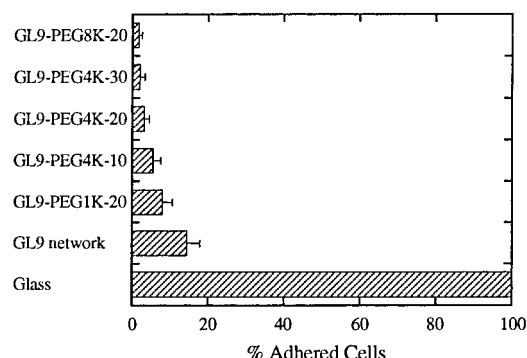


Figure 7. Fibroblast adhesion onto GL9-PEG networks.

to many months by changing the amount of L-lactide and PEG as well as the cross-linking density and by employing other biodegradable monomers such as glycolide or  $\epsilon$ -caprolactone for faster or slower degradation than with L-lactide, respectively.<sup>19</sup> Thus, these GL-PEG networks may be expected to be useful as scaffolds in tissue engineering development.

## Conclusions

New lactide-based poly(ethylene glycol) polymer networks have been prepared by UV polymerization using two nontoxic macromers, namely triacrylated oligolactide emanating from a glycerol center and monoacrylated PEG. All networks showed relatively low swelling and good bulk properties as compared to hydrogels. All networks had no melting endotherms and displayed glass transition temperatures indicative of phase-mixing of PEG. GL-PEG networks displayed chemical (by ESCA), physicochemical (by measures of wetting), and biological (by resistance to cell adhesion) evidence of the presence of PEG at the network surface, each of these diverse measures corroborating the others. High molecular weight PEG-Ac was more effective in exerting a surface influence than was lower molecular weight PEG. The grafting of bioactive ligands for specific cell adhesion and the preparation of porous scaffold having appropriate mechanical properties are presently under investigation to obtain polymer scaffolds for tissue engineering.

**Acknowledgment.** We wish to thank Dr. Young Ha Kim, Korea Institute of Science and Technology (KIST), for his valuable discussion and Donald L. Elbert, California Institute of Technology, for his technical assistance. This research was supported in part by NSF Grant BES-9696020 and NIH Grant HD 31462 and the Korea Science and Engineering Foundation (KOSEF).

## References and Notes

- (1) For reviews see: (a) Langer, R.; Vacanti, J. P. *Science* **1993**, *260*, 920. (b) Nerem, R. M.; Sambanis, A. *Tissue Eng.* **1995**, *1*, 3.
- (2) Hubbell, J. A.; Palsson, B. O.; Papoutsakis, E. T. *Biotechnol. Bioeng.* **1994**, *43*, 541 and 683.
- (3) Vacanti, C. A.; Mikos, A. G., Eds. *Tissue Eng.* **1995**, *1*, 147–228.
- (4) Hubbell, J. A.; Langer, R. *Chem. Eng. News* **1995**, March 13, 42.
- (5) Hubbell, J. A. *Bio/Technology* **1995**, *13*, 565.
- (6) Lysaght, M. J. *Tissue Eng.* **1995**, *1*, 221.
- (7) Langer, R.; Vacanti, J. P.; Vacanti, C. A.; Atala, A.; Freed, L. E.; Vunjak-Novakovic, G. *Tissue Eng.* **1995**, *1*, 151.
- (8) Kimura, Y.; Shirotani, K.; Yamane, H.; Kitao, T. *Macromolecules* **1988**, *21*, 3338.
- (9) Yoshida, M.; Asano, M.; Kumakura, M.; Katakai, R.; Mashimo, T.; Yuasa, H.; Yamanaka, H. *Eur. Polym. J.* **1991**, *27*, 325.
- (10) Ouchi, T.; Nozaki, T.; Okamoto, Y.; Shiratani, M.; Ohya, Y. *Macromol. Chem. Phys.* **1996**, *197*, 1823.
- (11) Barrera, D. A.; Zylstra, E.; Lansbury, P. T.; Langer, R. *J. Am. Chem. Soc.* **1993**, *115*, 11010; *Macromolecules* **1995**, *28*, 425.
- (12) Pierschbacher, M. D.; Ruoslahti, E. *Nature (London)* **1984**, *309*, 30.
- (13) Massia, S. P.; Hubbell, J. A. *J. Biol. Chem.* **1992**, *267*, 14019.
- (14) Massia, S. P.; Rao, S. S.; Hubbell, J. A. *J. Biol. Chem.* **1993**, *268*, 8053.
- (15) Cima, L. G. *J. Cell. Biochem.* **1994**, *56*, 155.
- (16) Amiji, M.; Park, K. *J. Biomater. Sci. Polym. Edn.* **1993**, *4*, 217.
- (17) Han, D. K.; Park, K. D.; Gyu, G. H.; Jeong, S. Y.; Kim, U. Y.; Min, B. G.; Kim, Y. H. *J. Biomed. Mater. Res.* **1996**, *30*, 23.
- (18) Han, D. K.; Jeong, S. Y.; Kim, Y. H.; Min, B. G.; Cho, H. I. *J. Biomed. Mater. Res.* **1991**, *25*, 561.
- (19) Sawhney, A. S.; Pathak, C. P.; Hubbell, J. A. *Macromolecules* **1993**, *26*, 581.
- (20) Fuerteges, F.; Abuchowski, A. *J. Controlled Release* **1990**, *11*, 139.
- (21) Drumheller, P. D.; Hubbell, J. A. *J. Biomed. Mater. Res.* **1995**, *29*, 207; *Anal. Biochem.* **1994**, *222*, 380.
- (22) Drumheller, P. D.; Hubbell, J. A. *J. Polym. Sci., Polym. Chem.* **1994**, *32*, 2715.
- (23) Han, D. K.; Hubbell, J. A. *Macromolecules* **1996**, *29*, 5233.
- (24) Du, Y. J.; Lemstra, P. J.; Nijenhuis, A. J.; van Aert, H. A. M.; Bastiaansen, C. *Macromolecules* **1995**, *28*, 2124.
- (25) Storey, R. F.; Wiggins, J. S.; Mauritz, K. A.; Puckett, A. D. *Polym. Compos.* **1993**, *14*, 17.
- (26) Argade, A. B.; Peppas, N. A. *Polym. Bull.* **1993**, *31*, 401.
- (27) Kim, S. H.; Han, Y. -K.; Kim, Y. H.; Hong, S. I. *Macromol. Chem.* **1992**, *193*, 1623.
- (28) Beamson, G.; Briggs, D. In *High Resolution XPS of Organic Polymers: The Scienta ESCA300 Database*; John Wiley: Chichester, England, 1992; pp 136–137.
- (29) Han, D. K.; Park, K. D.; Ahn, K. -D.; Jeong, S. Y.; Kim, Y. H. *J. Biomed. Mater. Res.: Appl. Biomater.* **1989**, *23* (A1), 87.
- (30) Han, D. K.; Jeong, S. Y.; Ahn, K. -D.; Kim, Y. H.; Min, B. G. *J. Biomater. Sci. Polym. Ed.* **1993**, *4*, 579.
- (31) Andrade, J. D.; Smith, L. M.; Gregonis, D. E. In *Surface and Interfacial Aspects of Biomedical Polymers, Vol. 1, Surface Chemistry and Physics*; Andrade, J. D., Ed.; Plenum: New York, 1985; pp 249–292.
- (32) Chaikoff, E. L.; Merrill, E. W.; Verdon, S. L.; Hayes, L. L.; Connolly, R. J.; Callow, A. D. *Polym. Commun.* **1990**, *31*, 182.
- (33) Llanos, G. R.; Sefton, M. V. *J. Biomater. Sci. Polym. Ed.* **1993**, *4*, 381.
- (34) Takahara, A.; Jo, N. J.; Kajiya, T. *J. Biomater. Sci. Polym. Ed.* **1989**, *1*, 17.
- (35) Lee, J. H.; Kopeckova, P.; Kopecek, J.; Andrade, J. D. *Biomaterials* **1990**, *11*, 455.
- (36) Chen, J. -H.; Stein, E. R. *J. Colloid Interface Sci.* **1991**, *142*, 545.
- (37) Takahara, A.; Jo, N. J.; Kajiya, T. *J. Biomater. Sci. Polym. Ed.* **1989**, *1*, 17.
- (38) Tseng, Y. C.; Park, K. *J. Biomed. Mater. Res.* **1992**, *26*, 373.
- (39) Sheu, M. S.; Hoffman, A. S.; Terlingen, J. G. A.; Feijen, J. *Polym. Prep.* **1991**, *32*, 239.